American Mineralogist, Volume 87, pages 753–764, 2002

The new mineral baumstarkite and a structural reinvestigation of aramayoite and miargyrite

HERTA EFFENBERGER,[1,*] WERNER HERMANN PAAR,[2] DAN TOPA,[2] ALAN J. CRIDDLE,[3] AND MICHEL FLECK[1]

[1]Institut für Mineralogie und Kristallographie, Universität Wien, Althanstrasse 14, A-1090 Vienna, Austria
[2]Institut für Mineralogie, Universität Salzburg, Hellbrunnerstrasse 34, A-5020 Salzburg, Austria
[3]Department of Mineralogy, The Natural History Museum, London SW7 5BD, U.K.

ABSTRACT

Baumstarkite is a new mineral found coating miargyrite from the San Genaro mine, Huancavelica Department, Peru. It is triclinic and the third naturally occurring modification of $AgSbS_2$ besides monoclinic miargyrite and cubic cuboargyrite. The composition is usually close to the ideal formula. However, some grains of baumstarkite show zoned lamellae with As contents up to 11.5 wt% and accords to $Ag_3(Sb,As)_2SbS_6$. Baumstarkite is isotypic with aramayoite [end-member composition $Ag_3Sb_2BiS_6$; solid solutions require the extended formula $Ag_3Sb_2(Bi,Sb)S_6$]. Single-crystal X-ray structure investigations were performed for baumstarkite [type locality, a = 7.766(2), b = 8.322(2), c = 8.814(2) Å, α = 100.62(2), β = 104.03(2), γ = 90.22(2)°, Z = 2{$Ag_3Sb_3S_6$}, space group $P\bar{1}$, R1(F) = 0.057, $wR_2(F^2)$ = 0.128], aramayoite [Armonia mine, El Quevar, Argentinia: a = 7.813(2), b = 8.268(2), c = 8.880(2) Å, α = 100.32(2), β = 104.07(2), γ = 90.18(2)°, Z = 2{$Ag_3Sb_2S_6$}, space group $P\bar{1}$, R1(F) = 0.034, wR2(F^2) = 0.084], and miargyrite associated with baumstarkite type material [a = 12.862(3), b = 4.409(1), c = 13.218(3) Å, β = 98.48(2)°, Z = 8{$AgSbS_2$}, space group $C2/c$, R1(F) = 0.031, wR2(F^2) = 0.082]. The space-group symmetries of aramayoite and miargyrite were revised, and the refinements unambiguously showed that the three investigated minerals are centrosymmetric.

In baumstarkite and aramayoite each three atomic sites are occupied by Ag and M = As, Sb, Bi, respectively. The Ag atoms have two short bonded ligands (Ag-S is 2.51 to 2.58 Å). The M1 and M2 sites are [3 + 3] coordinated and are predominantly occupied by (Sb, As) atoms (M-S = 2.44 to 2.54 Å and > 3.09 Å). The [2 + 2 + 2] coordination of the M3 atom differs in the two mineral species: the two shortest bond lengths in baumstarkite are smaller (2.51 Å) than in aramayoite (2.64 Å) to allow for the different sizes of the Sb and Bi atoms, respectively; the medium bond lengths are similar (2.75 to 2.82 Å) and the longest bond lengths are >3.02 Å. Considering only the nearest-neighbor environments, baumstarkite and aramayoite feature zigzag chains parallel to [010], which are linked together to form layers parallel to (001). In miargyrite [2 + 2] and [2] coordinated Ag atoms are linked by SbS_3 pyramids to form a three-dimensional network.

INTRODUCTION

Several minerals with the chemical formula $AgMS_2$ (M = As, Sb, Bi) have previously been described: (1) M = As: monoclinic smithite (Hellner and Burzlaff 1964), trigonal trechmannite (Matsumoto and Nowacki 1969); (2) M = Sb: monoclinic miargyrite (Hofmann 1938; Knowles 1964; Smith et al. 1997), cubic cubargyrite (Walenta 1998); and (3) M = Bi: (probably) trigonal matildite (Geller and Wernick 1959; Harris and Thorpe 1969). Schapbachite is identical with matildite and was discredited by Ramdohr (1938). In general these minerals have end-member compositions or show only minor substitutions at the M sites. The triclinic mineral aramayoite exhibits a partial solid solution M = (Sb, Bi) (Spencer 1926; Yardley 1926; Berman and Wolfe 1940; Mullen and Nowacki 1974). Although different type structures have been found for these minerals, many of the above cited authors mentioned the PbS (or rock salt) type as the parental structure (see also Graham 1951 and Wernick 1960). However, according to the classification of sulfosalts by Makovicky (1993) the type structures of the $AgMS_2$ minerals smithite, trechmannite, miargyrite, and aramayoite have to be considered as derivatives of the SnS archetype. High-temperature modifications are pseudocubic or cubic and tend to form solid solutions with galena (Wernick 1960); the low-temperature modifications feature distinct distortions caused by the crystal-chemical behavior of the cations. Except for cubargyrite, all these minerals have been known for many decades from a large number of localities and ore deposits. Partial knowledge of these minerals dates back to the 19th century. Miargyrite is an economically important Ag ore of many silver deposits, whereas aramayoite is rare and cubargyrite has been only documented in trace amounts. However, the available structural data for $AgMS_2$ compounds are limited. The semiconducting properties of the selenide and bismuth analogues are mentioned by Geller and Wernick (1959); the corresponding minerals are

* E-mail: herta.silvia.effenberger@univie.ac.at

bohdanowiczite, $AgBiSe_2$ (Banas et al. 1979), and volynskite, $AgBiTe_2$ (Bezsmertnaya and Soboleva 1965).

As part of an ongoing project on complex Ag-Sn mineralization in northwest-Argentinia (Paar et al. 1996, 2000) a suite of high-grade silver ore specimens from the San Genaro mine, Huancavelica Department, Castrovirreyna District, Peru, was investigated. One specimen composed of miargyrite was partially overgrown by small crystals and crystal aggregates of a mineral labeled "aramayoite." The crystals are triclinic, and most of them are twinned. Electron-microprobe analyses revealed a Bi-free $AgSbS_2$ composition, isochemical with miargyrite and cuboargyrite. Subsequent research proved isotypy with aramayoite. A limited solid solution is observed for M = (Sb, As) whereas aramayoite shows a partial solid solution for M = (Sb, Bi).

Possible further occurrences of baumstarkite are worth mentioning. (1) Kittel (1927) refers to two wet-chemical analyses of aramayoite from Chocaya, Bolivia, one of which exhibits As and Bi contents of 0.9 and 2.4 wt%, respectively. Recalculation of his analyses assuming admixed chalcopyrite and pyrite leads to a composition close to that of baumstarkite. (2) A triclinic phase with composition $AgSbS_2$ was reported as a rare associate of miargyrite from the abandoned Ag mine of Saint-Marie-aux-Mines, France (Saint Jaques vein, level –143 m, Giftgrube) by Bari (1982). (3) Sugaki and Kitakaze (1992) described a Bi-free "aramayoite" with As/(As + Sb) ratios between 0.08 and 0.28 from the epithermal quartz vein of the Koryu Au-Ag mine, Hokkaido, Japan.

The new mineral baumstarkite is named for the German mineralogist Manfred Baumstark (born 1954) who first provided crystals of "aramayoite" from San Genaro (MBB 98.36.01) for study purposes and drew attention to the occurrence of triclinic $AgSbS_2$ at Saint-Marie-aux-Mines. Both the mineral and the mineral name have been approved by the I.M.A. Commission of New Minerals and Mineral Names (no. 99-049). The holotype material is deposited at the Mineralogical Institute, University of Salzburg, Austria (catalogue nos. 14524, 14525) and at the Natural History Museum, London, U.K. (BM 2000,32 and 33). The present paper deals with the mineralogical description of baumstarkite. To facilitate the definition of baumstarkite and its chemical separation with respect to aramayoite, and to enable a structural comparison with miargyrite, the crystal structures of these two minerals were refined and their space-group symmetries were revised.

Occurrence and physical properties

Baumstarkite occurs as a rare constituent in high-grade Ag ores at the San Genaro mine, Huancavelica, Peru (Crowley et al. 1997). Among the associated minerals miargyrite is dominant; pyrargyrite, stannite, and kesterite are less frequent. Andorite, diaphorite, robinsonite, galena, chalcopyrite, sphalerite, and pyrite were found as trace components (identified by electron-microprobe analyses; see Fig. 1). Baumstarkite is of hypogene origin and was obviously precipitated from hydrothermal fluids with high activities of Ag, Sb, and S. Individual crystals do not exceed 3 mm in size. Crystal aggregates up to 40×10 mm coat miargyrite. Anhedral inclusions of baumstarkite in miargyrite up to several mm in diameter are common.

The megascopic color is iron-black but grayish-black on fresh surfaces. The streak is grayish-black, and the luster is metallic. Crystals of baumstarkite are opaque. In thin sections and at crystal edges baumstarkite is transparent and deep blood-red. The VHN_{25} ranges from 71.3–98.5 (mean 89.3) which corresponds roughly to a Mohs' hardness of 2.5. The cleavage is perfect parallel to {001} and less perfect parallel to {100}. Parting was not observed; the material is sectile, somewhat pliable, with an even fracture. The measured density is 5.33 g/cm^3 (as determined from a fragment weighing 20.43 mg by the Berman microbalance method) and corresponds with the calculated density of 5.39 g/cm^3. The habit is equant and the only crystallographic forms are pinacoids due to the crystal symmetry $\bar{1}$: {001}, {10$\bar{1}$}, {201}, {010}, and {01$\bar{1}$} are most frequent, and {100} is subordinate. The {001} form often represents cleavage faces. Twinning occurs occasionally, and the twin plane is (001) (Fig. 2); indexing is based on the orientation determined by X-ray investigations.

Optical properties

In plane-polarized reflected light individual grains of baumstarkite are weakly to moderately bireflectant from gray to white. The mineral is not pleochroic. Red internal reflections are uncommon in plane polarized light and occur only along fractures within the mineral where grains are very thin. However, strong fiery red internal reflections are abundant between crossed polars. The rotation tints of the most anisotropic grains are almost monochrome from bright white to gray (with a brownish tint) to a very dark blue. Other, less anisotropic grains, most of which are twinned, have vari-colored tints ranging from a dull greenish yellow through brown to mauve to dark blue. All of these properties are enhanced upon immersion in oil.

The visible spectrum reflectances of the mineral were measured at intervals of 10 nm (from 400 to 700 nm) with a Zeiss MPM 800 microscope spectrophotometer. The bandwidth of the grating monochromator was set at 5 nm, the effective numerical apertures of the 50× objectives used were limited to 0.28, the reflectance standard was WTiC (Zeiss 314), and the oil used for immersion measurements was Zeiss $N_D = 1.515$.

Test measurements were made on some weakly anisotropic grains. Their undispersed bireflectance values rarely exceeded 2% and corresponded closely to the higher reflectance values of the most anisotropic grain measured. The data collected from the latter (compared with data for aramayoite and miargyrite) are given in Table 1 and are shown graphically in Figure 3. Baumstarkite reveals monotone spectra for R_1 and R_2: in air the bireflectance is almost constant at 8% absolute, 22% relative, i.e., it is undispersed. The color values calculated relative to the standard illuminants A (2856 K) and C (6774 K) of the *International Commission on Illumination* (CIE 1971) show nearly constant dominant wavelengths (λ_d) or hue, and very weak excitation purities (P_e%) or saturation. It is apparent that differences in lightness (or luminance, Y%) alone that account for the perceived white-gray

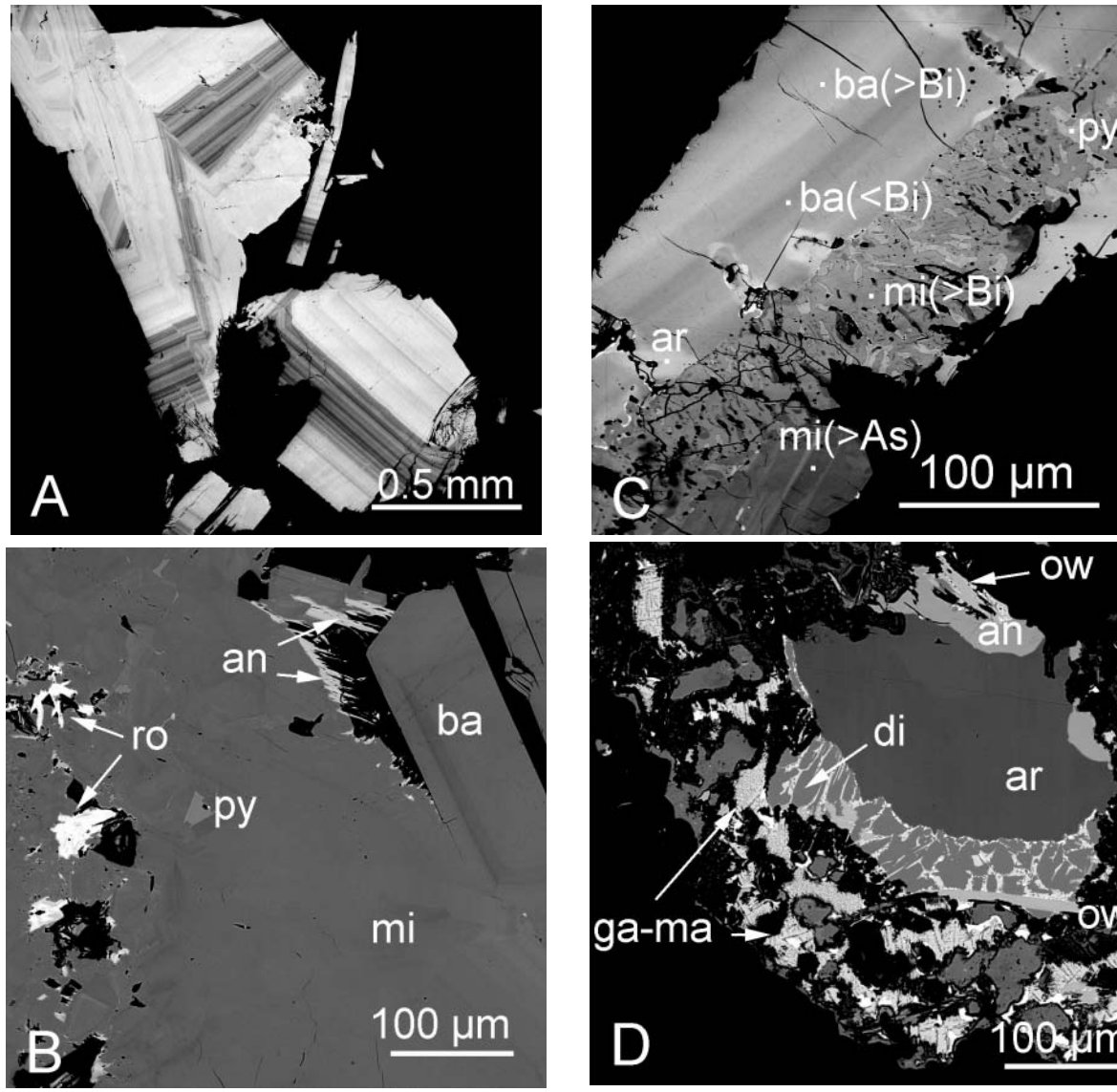

FIGURE 1. Backscattered electron images. (**a**) Fragments of baumstarkite with dark lamellae with high As content. (**b**) Baumstarkite crystals (ba) with weak compositional zonation and associated with miargyrite (mi), andorite (an), a robinsonite type material (ro), and traces of pyrargyrite (py). (**c**) Compositionally zoned baumstarkite, with local transition to aramayoite (ar), randomly intergrown with miargyrite (mi, Bi or As rich) and pyrargyrite (py). (**d**) Aramayoite with weak compositional zonation, surrounded (replaced) by a myrmekitic intergrowth of diaphorite (di) and galena-matildite s.s. (ga-ma) (lower part) and an andorite (an) like phase (upper part); owyheeite (ow) occurs as needle-shaped crystals penetrating the intergrowth. Samples in **a** and **b** are from San Genaro, Huancavelica (MBB 98.36.01, 99/49a-WHP301), **c** is from Pirquitas (Veta-vein Potosi; WHP1716), and **d** is from Armonia mine, El Quevar (EQ 95/9).

bireflectance. In oil, the ratio of the bireflectance is 6% absolute and 30% relative. When compared with the air values, it is the lower luminance values combined with the almost doubled relative values of excitation purity that explain the enhancement in the perceived bireflectance.

A polished sample of miargyrite associated with baumstarkite from the San Genaro mine, Huancavelica, Peru, was measured under the same conditions as the baumstarkite type specimen. The dispersion of the R_1 and R_2 and the $^{im}R_1$ and $^{im}R_2$ values closely match those of baumstarkite. In fact, although our data show the mineral to be less strongly bireflectant than baumstarkite, they also show that the R_2 and $^{im}R_2$ values for the two minerals are practically indistinguishable. It is, of course, not surprising that the optical properties of the two minerals are similar given their compositional similarity. The tabulated data for miargyrite match closely those of Caye and Pasdeloup (QDF3, 369,1993) for a sample from Hiendelaencina, Spain, while Picot and Johan's (1982) data for an unlocalized sample show that it is appreciably more bireflectant, and are a better fit for our data for baumstarkite. In the absence of compositional data in Picot and Johan's (1982) compilation, it is tempting to speculate that they mea-

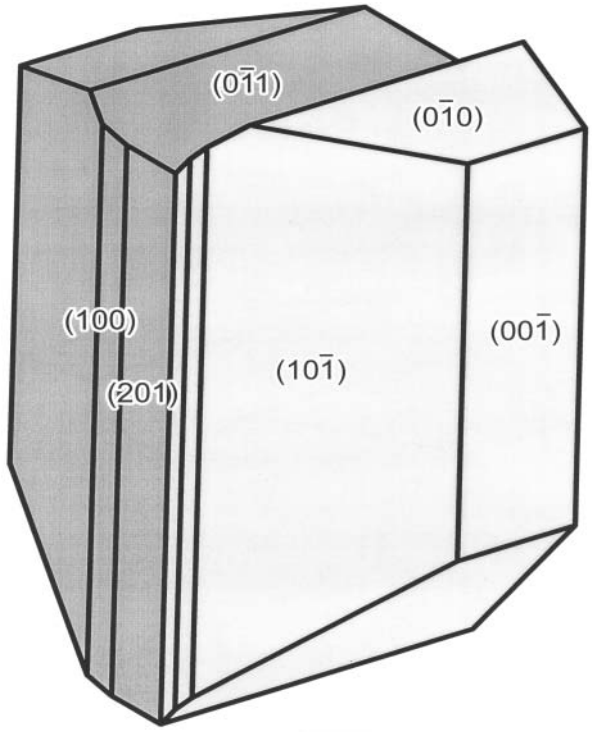

FIGURE 2. Sketch of a twinned crystal of baumstarkite; the twin plane is (001) (program SHAPE, Dowty 1999a).

sured a mineral nearer in composition to that of baumstarkite than miargyrite.

Our optical investigation of aramayoite revealed some interesting problems. The first sample studied, the type specimen (BM 1926,292) from the Animas mine in Bolivia, proved to be very weakly bireflectant and anisotropic. Other samples, including some from Portugalete, Bolivia (BM 1936,1160) and the Armonia mine, El Quevar, Salta Province, northwest Argentinia, conform more closely with the descriptions of Uytenbogaardt and Burke (1971) and Picot and Johan (1982) of a mineral with clearly defined cleavages parallel to twin lamellae. These differences in the reflectance and bireflectance between twins are accompanied by even stronger differences in anisotropic rotation tints. At a color temperature of ~3200 K the tints associated with the most anisotropic material vary from a reddish brown to a pale bright mauve to steel gray. Uytenbogaardt and Burke (1971) described the tints as light pink to steel blue, while Picot and Johan (1982) recorded orange-brown to green polarization colors. Color descriptions are notoriously inexact so how real these differences are is doubtful, however, spectral reflectance values from well-polished minerals should be more reliable. The reflectance data and color values of Caye and Pasdeloup (QDF3.15.1993) are a good fit for our data for the type specimen, but both of these sets of data are much lower in reflectance than those of Picot and Johan (1982). The probable explanation for these discrepancies was found when measurements were made of the Portugalete and Armonia mine samples. In both cases, the reflectance values could not be reproduced over a period of time. The wavelength scanning procedure we usually employ involves repeated measurement of the sample at 31 wavelengths in plane polarized light at orientations corresponding to extinction positions between crossed polars. This takes several minutes for each extinction position. The fact is that some samples of aramayoite are very light sensitive and that in the time taken to measure their reflectance spectra their reflectance values were falling. A revised procedure was adopted which involved the collection of data from single spectral scans on freshly polished surfaces. When this was done, the data collected from the Portugalete and Armonia mine samples were consistent. A representative set of data from the Armonia mine are included in Table 1 and Figure 3. Obviously, these differences are related to composition, allied perhaps to the structural orientation of grains and grain boundaries, but it is intriguing to note how light alone is enough to reveal them—it is also now quite clear why the reflectance spectra of this mineral measured on different samples should be approached with caution. Nevertheless, the spectra and color of aramayoite—even samples that have been affected to a limited extent by light—are different from those of miargyrite and baumstarkite, neither of which is in any case nearly as light sensitive.

CHEMICAL COMPOSITION

Quantitative chemical analyses of baumstarkite, aramayoite, and miargyrite were obtained by electron-microprobe (JEOL Superprobe JXA-8600, LINK-EXL software including an online ZAF correction, acceleration voltage of 25 kV with a beam current of 30 nA). The following natural and synthetic standards were used: stephanite (Ag$L\alpha$), stibnite (S$K\alpha$, Sb$L\alpha$), arsenopyrite (As$K\alpha$), and bismuthinite (Bi$L\alpha$). The results are compiled in Table 2.

Most crystals and grains of baumstarkite are almost pure Ag-Sb sulfides or contain minor amounts of arsenic. Trace amounts of Cu but no Bi were detected in the material available for study. However, several crystals contain sharply defined and chemically zoned lamellae (Figs. 1a and 1b) where As (up to 11.5 wt%) substitutes for Sb. The empirical formula of As-poor baumstarkite is based on the analytically detected values recalculated to a total of four apfu: $Ag_{0.99}(Sb_{0.97}As_{0.03})_{\Sigma=1.00}S_{2.01}$. The empirical formula matches well with the simplified formula $AgSbS_2$. From crystal structure refinements, the crystal chemical formula accounting for the partial solid solution between Sb and As is $Ag_3(Sb,As)_2SbS_6$.

Aramayoite was chemically characterized using samples originating from Bolivia (Animas mine, Chocaya), Argentinia (Armonia mine, El Quevar, Salta Province; Pirquitas mine, Jujuy Province), and Austria (Altenberg, Lungau District, Salzburg Province, Putz 2000). The material from Bolivia is from the type locality and represents co-type aramayoite (BM 1940,10), donated by the late Harry Berman to the Natural History Museum, London, U.K. All samples of aramayoite show a distinct substitution of Sb by Bi (Figs. 1c and 1d; Table 2). The Sb:Bi ratio is usually between ~3:1 to ~4:1, but it varies significantly at Pirquitas between ~4.4:1 and ~1.5:1,

TABLE 1. Reflectance measurements of baumstarkite, aramayoite, and miargyrite

	baumstarkite				aramayoite				miargyrite			
λ (nm)	R_1	R_2	$^{im}R_1$	$^{im}R_2$	R_1	R_2	$^{im}R_1$	$^{im}R_2$	R_1	R_2	$^{im}R_1$	$^{im}R_2$
400	33.15	40.95	19.20	25.95	38.90	43.40	23.60	25.92	37.30	39.80	22.00	24.90
420	32.70	40.75	18.40	25.25	38.85	42.50	23.70	26.20	37.10	40.00	21.85	24.95
440	32.15	40.20	17.60	24.30	38.50	41.90	23.40	26.10	36.90	39.45	21.55	24.40
460	31.60	39.65	17.00	23.80	38.40	41.60	23.00	25.50	36.50	39.05	21.10	23.85
480	31.10	39.50	16.40	23.30	38.20	41.10	22.85	25.35	35.85	38.60	20.35	23.35
500	30.40	38.80	15.80	22.60	38.05	40.90	22.65	24.80	34.95	38.05	19.45	22.60
520	29.95	38.10	15.25	21.80	37.80	40.50	22.40	24.50	34.05	37.30	18.60	21.90
540	29.35	37.40	14.70	21.30	37.50	40.25	22.10	24.20	33.30	36.55	17.95	21.20
560	28.60	36.80	14.10	20.75	37.30	40.05	21.80	24.00	32.75	35.90	17.40	20.50
580	28.10	36.45	13.65	20.50	37.10	40.10	21.50	23.90	32.10	35.30	16.80	19.95
600	27.60	35.70	13.20	19.80	37.00	40.10	21.40	23.85	31.30	34.75	16.20	19.50
620	27.05	34.65	12.80	18.85	36.70	39.90	21.10	23.60	30.55	34.00	15.50	18.75
640	26.45	33.60	12.30	17.90	36.60	39.50	20.85	23.40	29.90	33.20	14.90	18.00
660	25.90	32.70	11.95	17.25	36.20	39.10	20.55	22.90	29.25	32.35	14.40	17.30
680	25.45	32.40	11.75	16.60	36.10	39.00	20.00	22.30	28.80	31.85	14.05	16.85
700	25.15	31.25	11.70	16.30	36.30	39.80	20.20	22.50	28.60	31.55	13.95	16.75
						COM						
470	31.30	39.65	16.60	23.60	38.35	41.40	23.00	25.60	36.10	38.85	20.75	23.60
546	29.20	37.30	14.60	21.15	37.45	40.20	22.05	24.15	33.10	36.35	17.75	21.00
589	27.80	36.10	13.35	20.10	37.00	40.00	21.50	23.90	31.70	35.00	16.50	19.75
650	26.15	33.05	12.15	17.60	36.40	39.40	20.70	23.20	29.65	32.75	14.65	17.65
						CIE A						
x	0.435	0.436	0.424	0.428	0.444	0.445	0.440	0.438	0.434	0.436	0.423	0.428
y	0.405	0.407	0.402	0.405	0.407	0.406	0.406	0.408	0.405	0.406	0.402	0.404
Y%	28.40	36.40	13.90	20.40	37.20	40.10	21.70	20.60	32.30	35.55	17.03	20.20
λ_d	491	491	491	491	491	487	491	495	491	491	491	491
P_e%	3.1	2.8	5.8	4.6	0.85	0.8	1.8	2.3	3.4	2.8	6.0	4.9
						CIE C						
x	0.297	0.299	0.287	0.292	0.307	0.307	0.303	0.303	0.296	0.299	0.286	0.291
y	0.306	0.309	0.295	0.301	0.314	0.312	0.310	0.309	0.305	0.308	0.295	0.3
Y%	28.80	36.90	14.30	20.90	37.40	40.25	21.90	24.10	32.80	36.00	17.50	20.70
λ_d	480	482	479	480	487	475	481	476	480	481	479	480
P_e%	5.8	4.8	10.8	8.3	1.5	1.7	3.4	3.2	6.3	5.0	11.0	8.9

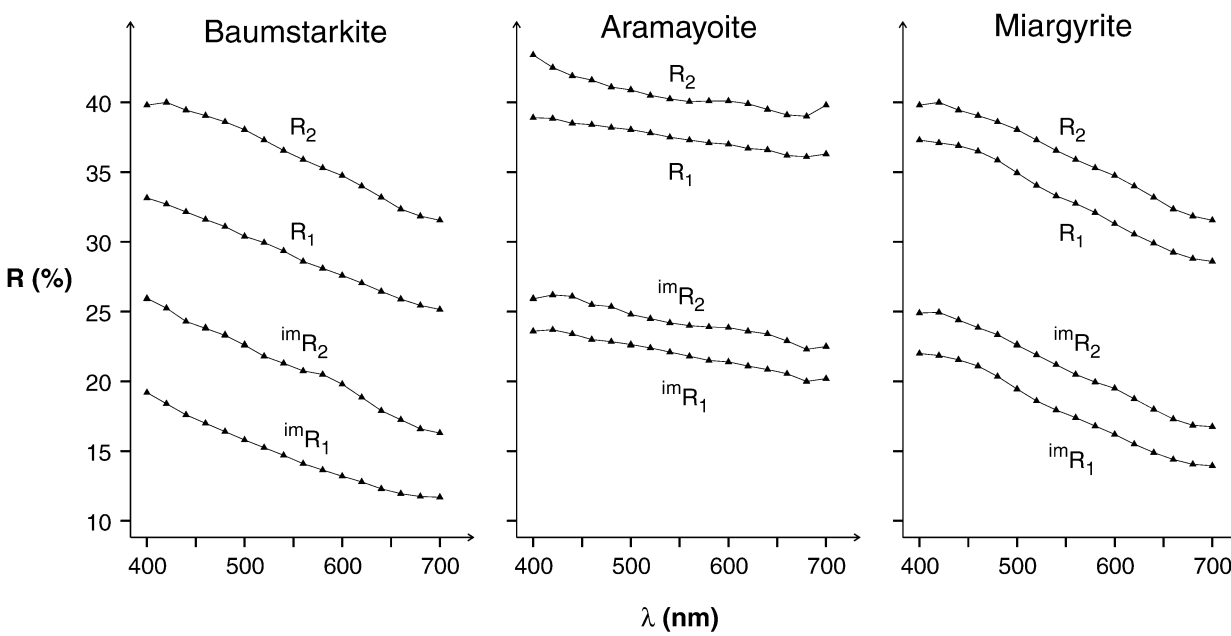

FIGURE 3. Reflectance spectra of baumstarkite, aramayoite, and miargyrite.

TABLE 2. Results of electron-microprobe investigations of baumstarkite and aramayoite

	N*	Ag	Sb	Bi	As	S	Total	Sb/Bi †
				baumstarkite				
San Genaro matrix (range) ‡	22	35.6–36.7	38.8–40.9		0.3–2.0	21.9–22.3		
San Genaro matrix (average)	22	36.3(3)	40.2(5)		0.7(4)	22.0(1)	99.4 §	
San Genaro lamellae 1	12	38.3(3)	27.9(17)		10.1(12)	23.1(2)	99.4	
San Genaro lamellae 2	14	37.4(3)	33.1(8)		6.2(5)	22.6(2)	99.3	
Pirquitas (range) ||	16	35.1–36.2	31.4 – 33.9	6.8 – 10.0	0.2 – 2.7	20.9 – 21.5		5.47 – 7.51
				aramayoite				
Chocaya (range, BM1940.10)	9	33.8–34.7	29.1–31.6	12.7–16.2	0.1–0.3	20.6–21.0		3.08–4.27
Chocaya (average, BM1136.1160)	9	34.3(3)	30.6(7)	14.1(1)	0.2(1)	20.8(1)	100.0	3.69
El Quevar (range) ‡	3	35.0–35.3	26.8–28.8	15.2–17.8	1.2–1.2	18.7–19.1		2.58–3.25
El Quevar (average)	3	35.1(2)	27.5(11)	16.3(13)	1.2(1)	18.9(2)	99.0	2.91
Pirquitas (range) #	20	32.9–36.8	21.8–30.5	11.9–25.0	0.2–0.9	19.5–20.9		1.44–4.41
Altenberg (average)	3	32.5(1)	22.6(6)	25.4(6)		19.5(1)	101.5**	1.5

* Number of analyses (values in wt%, standard deviations in parentheses).
† Ratio of atoms.
‡ A crystal out of these samples was used for X-ray investigations (EQ 95/9).
§ Included Cu 0.1 wt%.
|| Included Pb 0.4, Cu 0.2, Fe 0.6 wt%.
Included Pb 0.4–4.0, Cu 0.1–0.3, and Fe 0.1–0.6 wt%.
** Included Pb 1.33, Te 0.12 wt%.

and is ~1.5:1 at Altenberg. In two cases the ratio at Pirquitas is larger than 5.5:1, indicative of a more or less complete solid solution between aramayoite and baumstarkite. Samples with both As and Bi substituting for Sb on a larger scale have not yet been found.

Miargyrite associated with baumstarkite in the San Genaro mine was used for optical, chemical, and structural investigations (sample no. 00/10). Electron-microprobe analyses showed that all the grains are chemically inhomogeneous. The minor elements are Cu, As, Pb, and Hg. Copper and As vary between 0.12 and 0.16 wt% and between 0.4 and 1.5 wt%, respectively. Lead (between 0.8 and 2.86 wt%) was detected at seven, and Hg (between 0.3 and 2.2 wt%) at six of a total of nine points measured on several grains.

X-RAY INVESTIGATION

X-ray powder patterns of baumstarkite and aramayoite are similar and show very strong texture effects caused by the excellent cleavage of the minerals parallel to (001). The strongest lines detected are compared to those calculated from the structural parameters for baumstarkite in Table 3. Single-crystal X-ray structure investigations were performed from small crystal chips of baumstarkite, aramayoite, and miargyrite. Details of the structure refinements are compiled in Table 4, and final structural parameters are given in Table 5.

Baumstarkite. Single-crystal X-ray data collection was performed on the type material. The atoms were located by direct methods and difference Fourier maps. The refinement converged for space group $P\bar{1}$. The low anisotropy of the displacement parameters and the good agreement between the observed and calculated structure amplitudes supports centrosymmetry. The Ag and M atoms occupy three crystallographically independent atomic sites each. For the refinements the M sites were at first assumed to be fully occupied by Sb atoms. However, the equivalent isotropic displacement parameters indicated the possibility of a slightly smaller scattering power at the M2 site and a slightly higher one at the M3 site. Small amounts of As and Bi, respectively, substituting for Sb were considered.

Aramayoite. An earlier structural investigation of aramayoite by Mullen and Nowacki (1974) was not in agreement with the structure refinement of baumstarkite. Only the principle features of the atomic arrangements corresponded to each other, and some coordination polyhedra contradicted crystal chemical experience (e.g., Ag-S bond lengths of 2.05 and 2.11 Å). Despite a refinement of aramayoite in space group $P1$ by the former authors some sites were partially or mixed occupied. Mullen and Nowacki's (1974) faulty structure model was probably caused by the insufficient quality of their data: the accuracy of X-ray data available at that time (photographic non-integrated Weissenberg film data, multiple-film methods) was obviously overestimated. Their data did allow them to determine the structure type, but though they tried to deduce details on the order-disorder phenomena between Ag, Sb, and Bi they were unsuccessful. However, the main features of the structure were determined correctly.

To make a crystal-chemical comparison of the two isotypic mineral species a structure investigation of aramayoite was performed using material from different localities. The results compare well. The data presented in this paper were taken from a refinement of a sample from the Armonia mine, El Quevar, Argentinia, because of the higher accuracy of the structure refinement due to its better crystal quality. The struc-

TABLE 3. Comparison of X-ray diffraction powder patterns of baumstarkite and aramayoite (the six strongest peaks are listed)

			baumstarkite				aramayoite	
h	*k*	*l*	*d* (obs) (Å)	*I* (obs)	*d* (calc) (Å)	*I* (calc)	*d* (obs) (Å)	*I* (obs)
0	2	1	3.425	8	3.429	70	3.429	10
0	2	$\bar{2}$	3.258	3	3.259	58	3.247	17
2	0	$\bar{2}$	3.224	6	3.230	45	3.236	15
2	0	1	3.158	4	3.159	40	3.175	13
2	$\bar{2}$	1	2.841	8	2.844	80	2.842	29
2	2	$\bar{1}$			2.837	88		
0	0	3	2.798	100	2.802	100	2.814	100
2	2	2	2.013	5	2.013	28	2.021	8
2	2	$\bar{4}$	1.971	5	1.975	28	1.977	6
0	0	6	1.3994	6	1.4007	8	1.4073	7

Notes: Powder diffractometer data (Philips X'Pert diffractometer) (Cu$K\alpha_{1,2}$-radiation, internal standard Si). The powder diffraction pattern was calculated according to the results of structure refinements with the program LAZY PULVERIX (Yvon et al. 1977).

TABLE 4. Single-crystal X-ray data-collection and structure refinements

	baumstarkite	aramayoite	Miargyrite
Chemical formula	$Ag_3(Sb,As)_2SbS_6$	$Ag_3Sb_2(Sb,Bi)S_6$	$AgSbS_2$
a (Å)	7.766(2)	7.813(2)	12.862(3)
b (Å)	8.322(2)	8.268(2)	4.409(1)
c (Å)	8.814(2)	8.880(2)	13.218(3)
α (°)	100.62(2)	100.32(2)	–
β (°)	104.03(2)	104.07(2)	98.48(2)
γ (°)	90.22(2)	90.18(2)	–
V (Å³)	542 Å³	547 Å³	741 Å³
space group	$P\bar{1}$	$P\bar{1}$	*C*2/*c*
Z	2	2	8
δ_{calc} (g/cm³)	5.39	5.88	5.26
crystal dimensions (μm)	55 × 30 × 105	40 × 160 × 20	60 × 60 × 50
range of data collection (°)	5 < 2ϑ < 60	5 < 2ϑ < 60	5 < 2ϑ < 60
number of frames	413	445	425
scan time (s/°)	270	80	80
μ(Mo*K*α) (mm^{-1})	13.9	27.3	13.4
$R_{int} = \Sigma\|F_o^2 - F_o^2(mean)\|/\Sigma F_o^2$	0.077	0.030	0.058
$R1 = \Sigma(\|\|F_o\| - \|F_c\|\|)/\Sigma F_o$	0.057	0.034	0.031
$wR2 = [\Sigma w(F_o^2 - F_c^2)^2/\Sigma^{\circ} wF_o^4]^{1/2}$	0.128	0.084	0.082
extinction parameter absorption correction	0.0019(3)	0.0071(8)	0.0038(2)
transmission factors	crystal shape	crystal shape	crystal shape
observed unique reflections (n)	0.363 to 0.687	0.090 to 0.531	0.443 to 0.567
reflections with $F_o > 4\sigma(F_o)$	3147	3158	1080
variable parameters (p)	2867	3043	1002
$GooF = \{\Sigma[w(F_o^2 - F_c^2)^2]/(n-p)\}^{0.5}$	113	113	40
P_1	1.19	1.05	1.12
P_2	0.0239	0.0282	0.0343
max Δ/σ	11.95	4.73	3.94
final difference Fourier map (eÅ^{-3})	≤0.001	≤0.001	≤0.001
	–3.08 to +2.60	–0.87 to +1.09	–1.41 to +2.08

Note: NONIUS four-circle diffractometer equipped with a CCD detector and a fiber optics collimator, Mo tube, graphite monochromator, φ-scans for distinct ω-angles, Δφ = 2°/frame, frame size: binned mode, 621 × 576 pixels, detector-to-sample distance: 28 mm; range of data collection: ±*h* ±*k* ±*l*. Unit-cell parameters were obtained by least-squares refinements of accurate 2ϑ values. Corrections for Lorentz and polarization effects and absorption effects; neutral-atomic complex scattering functions (Wilson 1992), programs SHELXS-97, and SHELXL-97 (Sheldrick 1997a, 1997b). $\omega = 1 / \{\sigma^2(F_o^2) + [P_1{*}P]^2 + P_2{*}P\}$; $P = ([\max(0,F_o^2)] + 2{*}F_c^2) / 3]$.

tural refinement was begun using atomic coordinates obtained for baumstarkite. A markedly different occupation for the M sites was observed. The M1 and M2 sites are chiefly occupied by Sb atoms, and only small amounts of Bi substitute for the Sb atoms. However, the M3 site is predominately occupied by Bi atoms, with only small amounts of Sb. Our refinement clearly showed that aramayoite is centrosymmetric. No hints for a reduction of the space-group symmetry $P\bar{1}$ were found. The anisotropies of all the displacement parameters are unconspicuous. In addition, our results are in accordance with the chemical analyses of aramayoite which scatter around Ag:(Sb + Bi):S ratios of 3:3:6, but show a significant Bi content up to Bi:Sb = 1:2. In contrast, the structural formula derived by Mullen and Nowacki (1974) for aramayoite is $Ag_5Sb_{3.75}Bi_2S_{12}$ (based on structural data without a chemical analysis, the origin of the investigated samples is not mentioned).

Miargyrite. Miargyrite is isochemical with baumstarkite; therefore special attention was given to its crystal structure. The first examination based on Weissenberg-film data and packing considerations was performed by Hofmann (1938). Knowles (1964) found from single-crystal two-circle diffractometer data the extinction symbol *C*1*c*1 and tried refinements in space groups *C*2/*c* and *Cc*. Due to significant deviation of the atomic coordinates from centrosymmetry, and due to a lower *R* value, the authors finally described the crystal structure of miargyrite in the acentric space group *Cc*. Quite recently, Smith et al. (1997) reported on a structure refinement of miargyrite in space group *C*2. They mentioned the approximate *C*2/*c* symmetry, but found 60 reflections conflicting with the *c*-glide plane. Neither the method for detecting the reflections violating the extinction rule *h*0*l*: *l* = 2*n* (film methods or diffractometer data) nor the ratios I/σ_I were given. Smith et al. (1997) used a larger crystal than in the previous and present studies (0.15 × 0.13 × 0.11 mm) and a 8 kW rotating anode source for data collection. It cannot be excluded with certainty that the intensity of reflections violating the extinction conditions result from the λ/2 effect and/or from "Umweganregung" (Renninger reflections). Any significant deviation from centrosymmetry is not seen in their structure model.

A careful re-examination of the crystal structure of miargyrite gave no hints for a violation of the glide plane (the size of the crystal used was only 0.05 ↔ 0.06 ↔ 0.06 mm to reduce the absorption). The check of extinction rules was done using Weissenberg-film methods (Cu*K*α radiation) and a four-circle diffractometer. It is worth noting that even investigations with the CCD area detector and a conventional Mo tube operating at 1.9 kW gave no hint of violations of the extinction rule *h*0*l*: *l* = 2*n*; this method improves the ratio signal to background and consequently allows the recognition of weaker intensities as compared to conventional detectors. The structure refinements were performed in the three space groups *C*2/*c*, *Cc*, and *C*2. The resulting *R* values are practically the same, but both refinements in acentric space groups exhibit large elements in the correlation matrix. The symmetry reductions

cause an increase in the number of free variables from 40 in *C*2/*c* to 74 and 72 in *C*2 and *Cc*, which is not justified from the refinement. The anisotropy of the displacement parameters compares especially well in all three refinement models. Consequently the crystal structure of miargyrite is best described in the centrosymmetric space group *C*2/*c*.

RESULTS AND DISCUSSION

In baumstarkite, aramayoite, and miargyrite the environment of the Ag atoms is roughly characterized by the coordination numbers [2], [2 + 2], [4], or [2 + 2 + 2] (relevant interatomic bond lengths and bond angles are compiled in Table 6). Such coordinations are in agreement with common crystal chemical experience (Burdett and Eisenstein 1992). The gaps between the first and second coordination spheres differ but correlate with the shortest of the Ag-S bonds. Ag-S bond lengths begin for $Ag^{[2]}$ atoms at 2.39 Å, and for $Ag^{[2+2]}$/$Ag^{[4]}$/$Ag^{[2+2+2]}$ atoms between 2.51 and 2.58 Å. Additional S ligands exhibit a wide-spread distribution of bond distances. Most differences are in the environments of the Ag atoms in miargyrite: the Ag1 atom features four similar bond lengths, and the Ag2 atom has a distinct twofold-coordination with a huge gap to the next ligands. The S-Ag-S bond angles between the two nearest neighbors are 146° to 163°, but for the $Ag2^{[2]}$ atom in miargyrite the bond angle is 180° due to the site symmetry $\bar{1}$ of the central atom. Linear S-Ag-S bond angles between the two shortest bonds are rare.

An analysis of the displacement parameters of the Ag atoms shows that they correlate with the bond length distribution rather than with the S-$Ag^{[2]}$-S bond angles. The displacement of the Ag1 atom in miargyrite is relatively regular in accordance with the coordination figure which tends to a strongly distorted tetrahedron (principal mean-square atomic displacements of *U* are 0.045, 0.037, and 0.024 Å^2). In contrast, the Ag2 atom shows a large anisotropy. The principal mean-square atomic displacements of *U* are 0.070, 0.045, and 0.017 Å^2; the smallest axis is approximately in the direction of the two shortest bonds. This anisotropy might be considered as a possible reason for the lowering of the space-group symmetry *C*2/*c*. A reduction of the symmetries to both *C*2 or *Cc* abolishes site symmetry $\bar{1}$ and consequently allows a bent S-Ag2-S bond angle. However, refinements in both the acentric space groups result in structure models with anisotropies just as large as in the centrosymmetric model and therefore they do not justify a refinement in any lower symmetry. The anisotropy of the Ag2 atom in miargyrite is comparable to that of the Ag1 and Ag2 atoms in baumstarkite/aramayoite: the principal mean-square atomic displacements of *U* are 0.069, 0.066, 0.026/0.065, 0.057, 0.024 Å^2 and 0.069, 0.058, 0.028/0.070, 0.047, 0.025 Å^2. Consequently the anisotropy of the Ag1 atom in miargyrite should be considered as chiefly influenced by the pronounced gap between the two nearest and next ligands. The environments of the three Ag atoms in baumstarkite/aramayoite support that (1) mainly the bond-length distribution controls the anisotropy of the displacement parameters of the Ag atoms and that (2) the influence of a large or even linear angle S-$Ag^{[2]}$-S is minor. Despite the large S-$Ag3^{[2]}$-S angle of 163° the principal mean-square atomic displacements of *U* (0.047, 0.037, 0.030/0.039, 0.029, 0.025 Å^2) are comparable to that of the Ag1 atom in miargyrite. The other S-$Ag^{[2]}$-S angles scatter about 150°. In general, the shortest axes correspond with the directions of the shortest bonds. As in miargyrite, by way of trial a refinement of baumstarkite and aramayoite in space group *P*1 also resulted in large anisotropies of the displacement parameters of the sites Ag1 and Ag2.

In minerals with formula $AgMS_2$ the M = As, Sb, Bi atoms exhibit a one-sided nearest neighbor environment as characteristic for atoms with steric active lone-pair electrons. The displacement parameters indicate only moderate anisotropies for all the M atoms. Two different coordination geometries with different importance in sulfosalts were observed (Makovicky 1981, 1989). The M1 and M2 atoms in baumstarkite and aramayoite and the M atom in miargyrite show the usual [3 + 3] coordination. The sizes of the MS_3 pyramids are similar and indicate agreement with structural refinements, i.e., a predominant occupation by Sb atoms. Individual M-S bond lengths for the first coordination sphere are 2.44 to 2.54 Å, and the average bond lengths are 2.463 to 2.492 Å. Next ligands have M-S > 3.09 Å. However, a detailed comparison of the average bond distances in baumstarkite and aramayoite show moderate differences:

TABLE 5. Structural parameters (e.s.d.s in parentheses) for baumstarkite, aramayoite and miargyrite

atom	*x*	*y*	*z*	U_{equiv}
		baumstarkite		
Ag1	0.10810(16)	0.42584(14)	0.14892(15)	0.0536(3)
Ag2	0.29748(15)	0.07224(13)	0.84390(14)	0.0518(3)
Ag3	0.01456(12)	0.74128(12)	0.49807(10)	0.0377(3)
M1 = Sb	0.63539(8)	0.41859(7)	0.16628(7)	0.0218(2)
M2 = Sb	0.17282(8)	0.91999(7)	0.17039(7)	0.0217(2)
M3 = Sb	0.48601(8)	0.24662(7)	0.49470(8)	0.0239(2)
S1	0.8531(3)	0.2103(3)	0.2033(3)	0.0241(5)
S2	0.3751(3)	0.2545(3)	0.1731(3)	0.0242(5)
S3	0.7238(3)	0.5306(3)	0.4623(3)	0.0232(5)
S4	–0.0219(3)	0.7031(3)	0.1989(3)	0.0265(5)
S5	0.4430(3)	0.7655(3)	0.1869(3)	0.0239(5)
S6	0.2447(3)	1.0324(3)	0.4631(3)	0.0235(5)
		aramayoite		
Ag1	0.11503(12)	0.42287(9)	0.14742(10)	0.0485(2)
Ag2	0.30433(11)	0.07450(8)	0.84722(9)	0.0474(2)
Ag3	0.00914(7)	0.74334(7)	0.49858(6)	0.03067(17)
M1 = Sb	0.64238(5)	0.41787(4)	0.16524(4)	0.01789(15)
M2 = Sb	0.16700(5)	0.91841(4)	0.16979(4)	0.01789(15)
M3 = Bi	0.49374(3)	0.24679(3)	0.49421(3)	0.01903(10)
S1	0.85745(19)	0.20464(17)	0.20003(18)	0.0208(3)
S2	0.38019(19)	0.25024(18)	0.16822(17)	0.0200(3)
S3	0.73044(19)	0.52180(17)	0.46193(17)	0.0198(3)
S4	–0.02532(20)	0.69719(18)	0.19690(18)	0.0226(3)
S5	0.43666(19)	0.76178(18)	0.18244(17)	0.0198(3)
S6	0.23938(20)	1.02194(17)	0.46306(17)	0.0200(3)
		miargyrite		
Ag1	0.0	0.02945(14)	0.25	0.03479(17)
Ag2	0.0	0.5	0.5	0.04345(19)
M = Sb	0.25550(2)	–0.03358(7)	0.62662(2)	0.01811(14)
S1	0.14337(7)	0.3510(2)	0.69954(7)	0.0183(2)
S2	0.11173(7)	0.1796(2)	0.41767(7)	0.0212(2)

Notes: The anisotropic displacement parameters are defined as: $\exp[-2\pi^2\Sigma^3_{i=1}\Sigma^3_{j=1} U_{ij}\mathbf{a}^*_i\mathbf{a}^*_j h_i h_j]$, B_{eq} according to Fischer and Tillmanns (1988). The occupation factors were refined from scattering power by least-squares methods. Baumstarkite: Sb:As is 0.994(11):0.006(11) for M1 and 0.966(11):0.034(11) for M2, Sb:Bi is 0.974(6):0.026(6) for M3; aramayoite: Sb:Bi is 0.937(4):0.063(4), 0.963(4):0.037(4), and 0.097(5):0.903(5) for M1, M2, and M3.

TABLE 5.–*continued*

Atom	U_{11}	U_{22}	U_{33}	U_{23}	U_{13}	U_{12}
			baumstarkite			
Ag1	0.0526(6)	0.0438(6)	0.0660(7)	0.0089(5)	0.0186(5)	0.0228(5)
Ag2	0.0518(6)	0.0422(6)	0.0643(7)	0.0095(5)	0.0208(5)	–0.0126(5)
Ag3	0.0357(5)	0.0465(6)	0.0311(5)	0.0097(4)	0.0068(3)	0.0024(4)
M1	0.0232(3)	0.0183(3)	0.0247(4)	0.0046(2)	0.0070(2)	0.0027(2)
M2	0.0229(3)	0.0177(3)	0.0241(4)	0.0035(2)	0.0053(2)	0.0035(2)
M3	0.0248(4)	0.0193(4)	0.0272(4)	0.0018(2)	0.0073(2)	0.0020(2)
S1	0.0242(10)	0.0200(11)	0.0287(12)	0.0049(9)	0.0075(9)	0.0058(8)
S2	0.0237(10)	0.0241(11)	0.0251(11)	0.0057(9)	0.0063(8)	0.0002(8)
S3	0.0239(10)	0.0189(10)	0.0248(11)	0.0013(9)	0.0043(8)	0.0034(8)
S4	0.0266(11)	0.0223(11)	0.0305(12)	0.0025(9)	0.0087(9)	–0.0003(9)
S5	0.0252(10)	0.0219(11)	0.0254(11)	0.0051(9)	0.0072(8)	0.0064(8)
S6	0.0255(10)	0.0195(10)	0.0253(11)	0.0009(9)	0.0088(8)	0.0001(8)
			aramayoite			
Ag1	0.0479(4)	0.0414(4)	0.0565(4)	0.0060(3)	0.0156(3)	0.0205(3)
Ag2	0.0500(4)	0.0400(4)	0.0530(4)	0.0019(3)	0.0194(3)	–0.0170(3)
Ag3	0.0278(3)	0.0387(3)	0.0249(3)	0.0059(2)	0.0054(2)	0.0014(2)
M1	0.0182(2)	0.0163(2)	0.0195(2)	0.00364(14)	0.00499(14)	0.00172(13)
M2	0.0174(2)	0.0165(2)	0.0193(2)	0.00267(14)	0.00389(15)	0.00243(14)
M3	0.02031(14)	0.01733(14)	0.01897(14)	0.00252(9)	0.00456(9)	0.00126(8)
S1	0.0179(7)	0.0199(6)	0.0236(7)	0.0032(5)	0.0038(5)	0.0046(5)
S2	0.0185(7)	0.0224(7)	0.0187(7)	0.0037(5)	0.0039(5)	–0.0013(5)
S3	0.0199(7)	0.0190(6)	0.0189(6)	0.0007(5)	0.0035(5)	0.0011(5)
S4	0.0208(7)	0.0224(7)	0.0241(7)	0.0031(5)	0.0053(6)	–0.0021(5)
S5	0.0187(7)	0.0220(7)	0.0183(6)	0.0032(5)	0.0041(5)	0.0062(5)
S6	0.0208(7)	0.0198(6)	0.0185(6)	0.0001(5)	0.0053(5)	0.0012(5)
			miargyrite			
Ag1	0.0250(3)	0.0439(3)	0.0344(3)	0.0	0.0005(2)	0.0
Ag2	0.0346(3)	0.0593(4)	0.0392(4)	–0.0106(3)	0.0145(3)	0.0157(3)
Sb	0.0218(2)	0.0184(2)	0.0148(2)	–0.00050(8)	0.00464(12)	–0.00022(9)
S1	0.0180(4)	0.0203(5)	0.0170(4)	–0.0004(3)	0.0041(3)	–0.0005(3)
S2	0.0207(4)	0.0237(5)	0.0210(4)	0.0017(3)	0.0084(3)	0.0012(4)

<M1-S> and <M2-S> are both slightly but significantly larger in aramayoite (2.489 and 2.475 Å) than in baumstarkite (2.472 and 2.463 Å). This behavior is in accordance with the partial substitution of Sb by As and Bi atoms in the two minerals, respectively.

In baumstarkite and aramayoite, the positions M3 = Sb and Bi feature a distinct environment with coordination number [2 + 2 + 2]. Furthermore, a huge difference in the short M3-S bond lengths is observed for the two minerals due to the predominant occupation by Sb and Bi atoms, respectively. The shortest and medium M3-S bond lengths in baumstarkite (~2.51 and 2.76 Å) are smaller than in aramayoite (~2.64 and 2.81 Å) to allow for the different size of the Sb and Bi atoms, respectively. Two further ligands are at a distance of ~3.0 Å indicating only moderate chemical interactions. It is worth mentioning that these fifth and sixth M3-S bond lengths are larger for baumstarkite than for aramayoite. This causes a stronger distortion for the $M3S_6$ polyhedron in baumstarkite (BiS_6) than in aramayoite (SbS_6). Probably steric reasons caused by the structure type are responsible for the reverse of the Bi-S/Sb-S bond lengths. In addition, the steric activity of the lone-pair electrons of the Sb^{3+} atoms seems to be more pronounced as compared to Bi^{3+} atoms.

The different size of the coordination of the M atoms reflects the chemical variability of baumstarkite and aramayoite. Despite ideal compositions of $Ag_3Sb_3S_6$ and $Ag_3Sb_2BiS_6$, extensive substitution between As:Sb and Sb:Bi was found by chemical analysis. Due to the different size and geometry of the $M1^{[3]}S_3$ and $M2^{[3]}S_3$ pyramids compared to the $M3^{[2+2]}S_4$ polyhedra any significant As content substitutes for Sb at the M1 and M2 position whereas the M3 position is occupied either by Sb or by Bi atoms. Only small amounts of Bi substituting for Sb at the M1 and M2 position in aramayoite were observed. Both three and four ligands in the first coordination sphere of Sb and Bi atoms are known, whereas $As^{[4]}$ is uncommon (for an exception see bernardite, $TlAs_5S_8$, Pašava et al. 1989). Consequently, the crystal chemical formula for the structure type is roughly $Ag_3(As,Sb)_2(Sb,Bi)S_3$. In approximate accordance with these crystal-chemical considerations, the analytically determined Sb:Bi ratio in aramayoite is ≥1.8:1.2 and the Sb:As ratio in baumstarkite is ≥ 1.9:1.1. Considering the limiting ratios Sb:Bi ≥2.0:1.0 and Sb:As ≥1.0:2.0, the compositions of baumstarkite and aramayoite are $Ag_3(Sb,As)_2SbS_3$ and $Ag_3Sb_2(Bi,Sb)S_3$, respectively. However, samples of baumstarkite with small contents of both As and Bi according to $Ag_3(Sb_{0.95}As_{0.05})_2(Sb_{0.9}Bi_{0.1})S_3$ were also detected (Table 2).

STRUCTURAL RELATIONSHIPS

Authors of earlier papers dealing with X-ray work on $AgMS_2$ minerals have considered structural relations within this group of compounds from the point of view of cell metrics, strongest lines in the powder pattern, and from structural investigations (as far as they were available). Previous papers mentioned the PbS type as the parental structure. Additionally, this structural relation has been deduced from the phase transitions. Cubic high-temperature modifications of $AgMS_2$ are described as crystallizing in the PbS type; Ag and M atoms are octahedrally coordinated and statistically occupy one atomic site. The low-temperature modifications of these compounds exhibit complete ordering of Ag and M atoms. Order phenomena are

TABLE 6. Interatomic bond distances (in Å) and bond angles (in E) for baumstarkite (M1 = M2 = M3 = Sb) and aramayoite (M1 = Sb, M2 = Sb, M3 = Bi) and miargyrite

bond distances	baumstarkite	aramayoite	bond angles	baumstarkite	Aramayoite
Ag1–S2	2.510(3)	2.508(2)	S2-Ag1-S4	149.29(10)	151.35(6)
Ag1-S4	2.529(3)	2.536(2)			
Ag1-S1[2]	2.849(3)	2.874(2)			
Ag1-S4[7]	2.964(3)	2.948(2)			
Ag2-S5[11]	2.518(3)	2.523(2)	S5[11]-Ag2-S1[8]	145.70(9)	147.79(6)
Ag2-S1[8]	2.540(3)	2.545(2)			
Ag2-S4[9]	2.849(3)	2.889(2)			
Ag2-S2[5]	2.934(3)	2.877(2)			
Ag2-S6[4]	3.235(3)	3.273(2)			
Ag3-S1[11]	2.538(3)	2.581(2)	S1[11]-Ag3-S4	163.01(9)	162.74(5)
Ag3-S4	2.542(3)	2.584(2)			
Ag3-S3[2]	2.774(3)	2.760(2)			
Ag3-S6[19]	2.801(3)	2.786(2)			
Ag3-S3[11]	3.058(3)	3.004(2)			
Ag3-S6	3.109(3)	3.025(2)			
M1-S1	2.436(2)	2.447(2)	S1-M1-S2	97.69(8)	97.26(5)
M1-S2	2.454(3)	2.478(2)	S1-M1-S3	89.55(8)	88.98(5)
M1-S3	2.525(3)	2.541(2)	S2-M1-S3	95.35(8)	95.14(5)
M1-S5[10]	3.118(3)	3.089(2)			
M1-S5	3.251(3)	3.269(2)			
M1-S4[1]	3.479(3)	3.395(2)			
M2-S4	2.437(3)	2.445(2)	S4-M2-S5	97.44(8)	97.18(6)
M2-S5	2.453(2)	2.466(2)	S4-M2-S6	91.40(9)	90.43(5)
M2-S6	2.500(3)	2.513(2)	S5-M2-S6	93.80(9)	93.61(5)
M2-S2[3]	3.185(3)	3.209(2)			
M2-S1[10]	3.229(3)	3.218(2)			
M2-S1[6]	3.496(3)	3.413(2)			
M3-S3[11]	2.510(2)	2.639(2)	S3[11]-M3-S6[4]	90.67(8)	89.08(5)
M3-S6[4]	2.511(2)	2.647(2)	S3[11]-M3-S5[11]	89.33(8)	88.31(5)
M3-S5[11]	2.747(3)	2.803(2)	S3[11]-M3-S2	86.86(8)	87.47(5)
M3-S2	2.769(3)	2.819(2)	S6[4]-M3-S5[11]	85.04(8)	85.08(5)
M3-S3	3.090(3)	3.023(2)	S6[4]-M3-S2	89.94(8)	89.35(5)
M3-S6[11]	3.144(3)	3.062(2)	S5[11]-M3-S2	173.67(7)	173.07(4)
miargyrite					
Ag1-S2[0,13]	2.5448(11)		S2[0]-Ag1-S2[13]	149.82(5)	
Ag1-S1[12,14]	2.6498(10)		S2[0,13]-Ag1-S1[12,14]	93.40(3)	105.68(3)
Ag1-S1[9,17]	3.4169(11)		S1[12]-Ag1-S1[14]	101.49(5)	
Ag2-S2[0,9]	2.3888(9)		S2[0]-Ag2-S2[9]	180	
Ag2-S1[0,9]	3.0587(11)				
Ag2-S2[3,12]	3.5626(11)				
Sb-S2[17]	2.4471(10)		S2[17]-Sb-S1	97.00(4)	
Sb-S1	2.5082(9)		S2[17]-Sb-S1[13]	93.57(3)	
Sb-S1[18]	2.5199(10)		S1-Sb-S1[18]	92.00(3)	
Sb-S2	3.2289(12)				
Sb-S1[4]	3.2835(11)				
Sb-S2[15]	3.4157(11)				

Notes: Symmetry code: 0 = *x y z* (if specified in cases of multiple bonds); 1 = *x* + 1, *y*, *z*; 2 = *x* – 1, *y*, *z*; 3 = *x*, *y* + 1, *z*; 4 = *x*, *y* – 1, *z*; 5 = *x*, *y*, *z* + 1; 6 = *x* – 1, *y* + 1, *z*; 7 = –*x*, –*y* + 1, –*z*; 8 = –*x* + 1, –*y*, –*z* +1; 9 = –*x*, –*y* + 1, –*z* + 1; 10 = –*x* + 1, –*y* + 1, –*z*; 11 = –*x* + 1, –*y* + 1, –*z* + 1; 12 = –*x*, –*y*, –*z* + 1; 13 = –*x*, *y*, –*z* + $^1/_2$; 14 = *x*, –*y*, *z* + $^1/_2$; 15 = –*x* + $^1/_2$, –*y* – $^1/_2$, –*z* + 1; 16 = –*x* + $^1/_2$, –*y* + $^1/_2$, –*z* + 1; 17 = *x*, –*y* + 1, *z* – $^1/_2$; 18 = –*x* + $^1/_2$, *y* – $^1/_2$, –*z* + $^3/_2$; 19 = –*x*, –*y* + 2, –*z* + 1.

accompanied by distinct coordinations. The M atoms have one-sided coordinations due to the steric activity of their lone-pair electrons. Consequently the relation to the PbS type is only a rough description. The differences in the M-S bonds no longer justify an approximation by sixfold coordination. According to detailed investigations of sulfosalts by Makovicky (1993) the type structure of the $AgMS_2$ minerals should be considered as derivatives of the SnS archetype to account for their special coordinations and the bond-strength distributions. Despite the derivation from one structure type, the linkage among the short connected atoms in the $AgMS_2$ minerals is different.

Considering only the nearest-neighbor environment, the type structure of the two isotypic minerals baumstarkite and aramayoite comprises zigzag chains parallel to [010] with formula $\{AgMS_2\}$ (Fig. 4). The MS_3 pyramids are corner-connected to MS_4 polyhedra; MS_3 pyramids share two corners with MS_4 polyhedra and MS_4 shares four corners with MS_3 pyramids. M-S_{shared} is longer than M-$S_{unshared}$. The S atoms making short bonds to only one M atom (S1 and S4) make two $Ag^{[2]}$-S bonds. Two of the S atoms sharing corners between MS_3 and MS_4 polyhedra are involved in one $Ag^{[2]}$-S bond (S2 and S5) whereas S3 and S6 are only weakly connected to Ag atoms. All $Ag^{[2]}$-S bonds are within the chains. The chains are interconnected by additional Ag-S and M-S bonds to layers parallel to (001). The Ag-S bonds between the layers are >2.93 Å, in agreement with the observed cleavage (see Fig. 5). Following Mullen and Nowacki (1974) and Graham (1951), one of the (001) layers in baumstarkite and aramayoite might be seen as three sheets

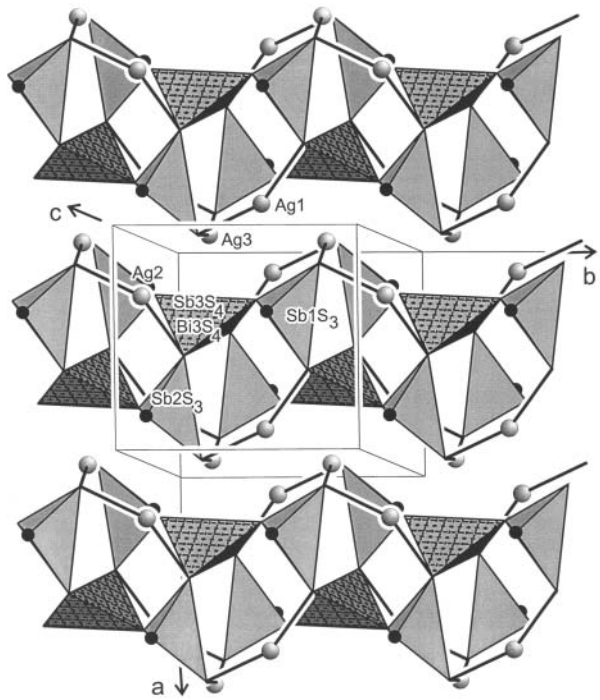

FIGURE 4. The zigzag $^{1}_{\infty}\{AgMS_2\}$ chains running parallel to [010] in the crystal structures of baumstarkite and aramayoite and their stacking within the (001) plane. The Ag atoms and the Ag-S bonds <2.60 Å are shown. The SbS_3 pyramids are shaded, and the SbS_4 and BiS_4 polyhedra are cross hatched (all structural drawings used the ATOMS program, Dowty 1999b).

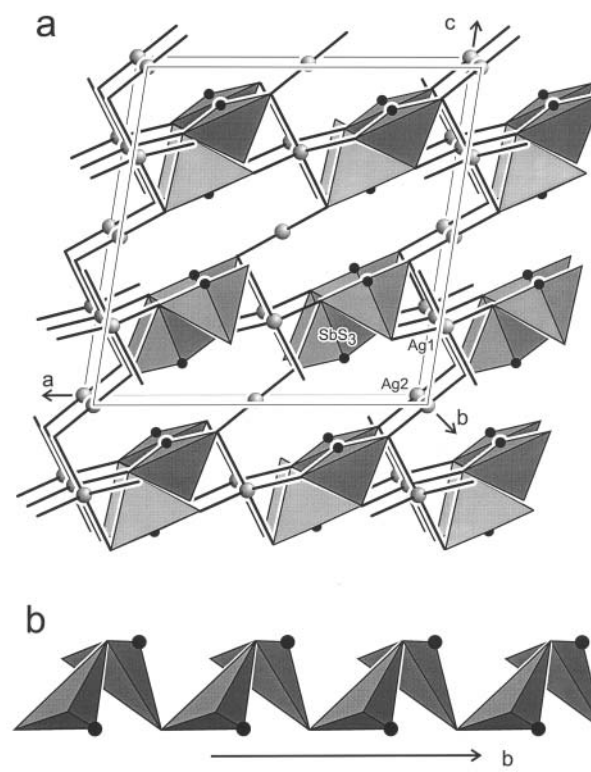

FIGURE 6. The crystal structure of miargyrite: (**a**) For Ag atoms nearest neighbor environment with Ag-S bond lengths <2.70 Å is shown. The SbS_3 pyramids are shaded. (**b**) One $^{1}_{\infty}\{SbS_2\}$ chain formed by the SbS_3 pyramids running parallel to the **b** axis.

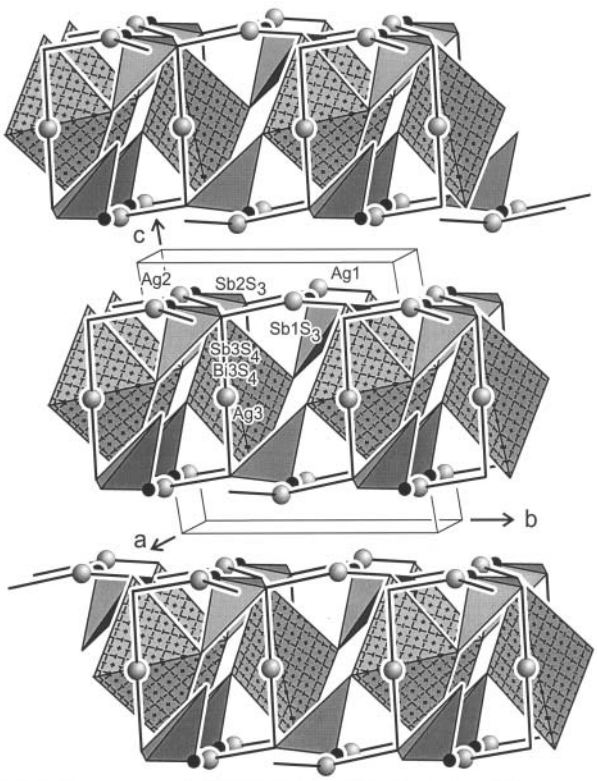

◀ **FIGURE 5.** The crystal structure of baumstarkite and aramayoite. The Ag atoms with their two nearest neighbors are shown. The SbS_3 pyramids are shaded, and the SbS_4 and BiS_4 polyhedra are cross hatched.

of a distorted PbS type structure.

Miargyrite is formed by chains of corner connected SbS_3 pyramids running parallel to [010] (Figs. 6a and 6b). The M-S bonds with the shared S1 atoms are longer than those with the unshared S2 atoms. The $\{MS_2\}$ chains are linked by $Ag1^{[4]}$ and $Ag2^{[2]}$ atoms. The structural relation of miargyrite and the PbS type have been described by many authors. Knowles (1964) mentioned that only the cations correlate with the PbS structure whereas the S atoms are greatly displaced. According to Makovicky (1993) the type structure of miargyrite is deduced from a periodically twinned SnS-like array. The cell volumes recalculated for one $AgSbS_2$ unit indicate distinct packing densities. Miargyrite (92.9 $Å^3$) is less densely packed as compared to baumstarkite (90.3 $Å^3$) and cubargyrite (90.2 $Å^3$; Walenta 1998). It is worth mentioning that aramayoite has a volume of only 91.2 $Å^3$ for one $AgSb_{2/3}Bi_{1/3}S_2$ unit, i.e., less than miargyrite.

ACKNOWLEDGMENTS

W.H.P. is especially thankful to the Austrian Research Council (FWF) for providing financial support through grants P 11987 GEO and P 13974 GEO. Financial support by the International Centre for Diffraction Data is gratefully acknowledged (Grant 90/03 ET). We acknowledge technical assistance by W. Waldhör during preparation of polished sections for microprobe analysis. The authors thank R.C. Peterson and M.F. Fleet for helpful comments and remarks that improved the manuscript.

REFERENCES CITED

Banas, M., Atkin, D., Bowles, J.F.W., and Simpson, P.R. (1979) Definitive data on bohdanowiczite, a new silver bismuth selenide. Mineralogical Magazine, 43, 131–133.

Bari, H. (1982) Minéralogie des filons du Neuenberg a Sainte Marie-aux-Mines (Haut-Rhine). Pierres et Terre 23–24, 70–71.

Berman, H. and Wolfe, C.W. (1940) Crystallography of aramayoite. Mineralogical Magazine, 25, 466–473.

Bezsmertnaya, M.S. and Soboleva, L.N. (1965) Volynskite, a new telluride of bismuth and silver. Eksperimentalno Metod. Issled. Rudnykh Mineralov, 1965, 129–141.

Burdett, J.K. and Eisenstein, O. (1992) From three- to four-coordination in copper(I) and silver(I). Inorganic Chemistry, 31, 1758–1762.

Caye, R. and Pasdeloup, J. (1993) pages 15 and 369, in A.J. Criddle and C.J. Stanley (eds.) The Quantitative Data File for ore minerals. The Commision on Ore Mineralogy, International Mineralogical Association. 699 p. Chapman & Hall, London.

CIE (1971) Colorimetry. Official Recommendations of International Commission on Illimination, Publication CIE No. 15 (E-1.3.1.). Bureau Central de la CIE, Paris.

Crowley, J.A., Currier, R.H., and Szenics, T. (1997) Mines and Minerals of Peru, 87–94: Huancavelica Group. Mineralogical Record, 28/4, 7–98.

Dowty, E. (1999a) SHAPE 6.0. Professional edition. A Computer Program for Crystal Morphology. Kingsport, TN 37663, USA.

———(1999b) ATOMS 5.0. A Computer Program for Atomic-Structure Display. Kingsport, TN 37663, USA.

Fischer, R.X., and Tillmanns, E. (1988) The equivalent isotropic displacement factor. Acta Crystallographica, C44, 775–776.

Geller, S. and Wernick, H.J. (1959) Ternary semiconducting compounds with sodium chloride-like structure: $AgSbS_2$, $AgSbTe_2$, $AgBiS_2$, $AgBiS_2$. Acta Crystallographica, 12, 46–54.

Graham, A.R. (1951): Matildite, aramayoite, miargyrite. American Mineralogist, 36, 436–449.

Harris, D.C. and Thorpe, R.I. (1969) New observations on matildite. Canadian Mineralogist, 9, 655–662.

Hellner, E. and Burzlaff, H. (1964) Die Struktur des Smithits $AgAsS_2$. Die Naturwissenschaften, 51, 53–54.

Hofmann, W. (1938) Die Struktur von Miargyrit $AgSbS_2$. Sitzungsberichte der Preußischen Akademie der Wissenschaften, Sitzung der physikalisch-mathematischen Klasse, 111–119.

Kittel, E. (1927) Aramayoite, un nuevo mineral de Bolivia. Revista Minera de Bolivia, Oruro, 2, 53–57.

Knowles, Ch.R. (1964) A redetermination of miargyrite, $AgSbS_2$. Acta Crystallographica, 17, 847–851.

Makovicky, E. (1981) The building principles of bismuth-lead sulphosalts and related compounds. Fortschritte Mineralogie, 59, 137–190.

———(1989) Modular classification of sulfosalts-current status. Definition and application of homologous series. Neues Jahrbuch für Mineralogie, Abhandlungen, 160, 269–297.

———(1993) Rod-based sulphosalt structures derived from the SnS and PbS archetypes. European Journal for Mineralogy, 5, 545–591.

Matsumoto, T. and Nowacki, W. (1969) The crystal structure of trechmannite, $AgAsS_2$. Zeitschrift für Kristallographie, 129, 163–177.

Mullen, D.J.E. and Nowacki, W. (1974) The crystal structure of aramayoite $Ag(Sb,Bi)S_2$. Zeitschrift für Kristallographie, 139, 54–69.

Paar, W.H., Brodtkorb, M.K.de, Topa, D., and Sureda, R.J. (1996) Caracterización mineralógica y chímica de algunas especies metalíferas de yacimiento Pirquitas, Provincia de Jujuy, República Argentinia: Parte 1. XIII Congreso Geológico y III Congreso de Exploracíon de Hidrocarburos, Actas III, 159–172.

Paar, W.H., Miletich, R., Topa, D., Criddle, A.J., Brodtkorb, M.K.de, Amthauer, G., and Tippelt, G. (2000) Suredaite, $PbSnS_3$, a new mineral species, from the Pirquitas Ag-Sn deposit, NW-Argentina: Mineralogy and crystal structure. American Mineralogist, 85, 1066–1075.

Pašava, J., Pertlik, F., Stumpfl, E.F., and Zemann, J. (1989) Bernardite, a new thallium arsenic sulphosalt from Allchar, Macedonia, with a determination of the crystal structure. Mineralogical Magazine, 53, 531–538.

Picot, P. and Johan, Z. (1982) Atlas of ore minerals. 458 p. B.R.G.M. Elsevier, Amsterdam.

Putz, H. (2000) Lagerstättenmineralogie von edelmetallführenden Vererzungen im Altenbergtal, Silbereck Formation, Lungau, Salzburg. Thesis, University Salzburg, 133 p.

Ramdohr, P. (1938) Über Schapbachit, Matildit und den Silber- und Wismutgehalt mancher Bleiglanze. Sitzungsberichte der Preußischen Akademie der Wissenschaften, Sitzung der physikalisch-mathematischen Klasse, 71–91.

Sheldrick, G.M. (1997a) SHELXS-97, a program for for the solution of crystal structures. University Göttingen, Germany.

———(1997b) SHELXL-97, a program for crystal structure refinement. University Göttingen, Germany.

Smith, J.V., Pluth, J.J., and Shao-xu Han (1997) Crystal structure refinement of miargyrite, $AgSbS_2$. Mineralogical Magazine, 61, 671–675.

Spencer, L.J. (1926) Aramayoite, a new mineral from Bolivia. Mineralogical Magazine, 21, 156–162.

Sugaki, A. and Kitakakaze, A. (1992) Discovery of As analogue of aramayoite and its phase relations in the Ag_2S–As_2S_3–Bi_2S_3–Sb_2S_3 join. 29th International Geological Congress, Kyoto, Japan, Abstracts, 673.

Uytenbogaardt, W. and Burke, E.A.J. (1971) Tables for microscopic identification of ore minerals, 430 p. Elsevier, Amsterdam.

Wernick, J.H. (1960) Constitution of the $AgSbS_2$–PbS, $AgBiS_2$–PbS, and $AgBiS_2$–$AgBiSe_2$ systems. The American Mineralogist, 45, 591–598.

Walenta, K. (1998) Cuboargyrite, ein neues Silbermineral aus dem Schwarzwald. Lapis, 23/11, 21–23.

Wilson, A.J.C., Ed. (1992) International tables for crystallography, vol. C, mathematical, physical and chemical tables, 883 p., Kluwer, Dordrecht.

Yardley, K. (1926): X-ray examination of aramayoite. Mineralogical Magazine, 21, 163–168.

Yvon, K., Jeitschko, W., and Parthé, E. (1977) LAZY PULVERIX, a computer program, for calculating X-ray and neutron powder diffraction patterns. Journal of Applied Crystallography, 10, 73–74.

MANUSCRIPT RECEIVED APRIL 16, 2001
MANUSCRIPT ACCEPTED JANUARY 3, 2002
MANUSCRIPT HANDLED BY MICHAEL E. FLEET